韓國産業應用學會誌, 제5권, 제3호, 233-238, 2002.8
J. Korean Society of Industrial Application, Vol.5, No.3, 233-238, Aug, 2002

입력주파수 변화에 따른 유도가열조리기의 자계-열계 해석에 관한 연구

A Study on the Magneto-Thermal Analysis of Induction Heating Jar according to Input Frequency Variation

오홍석*
Hong-Seok Oh*

<요 약>

본 논문에서는 유도가열조리기의 효과적인 설계를 위하여 입력주파수 변화에 따른 유도가열조리기의 자계와 열계 해석 방법을 제시하였다. 유도가열조리기의 내부자계는 3차원 축대칭 유한요소법을 사용하여 해석하였으며, 열원은 유도가열조리기의 내부에서 유도된 와전류에 의하여 발생되고, 열은 열원과 열방정식을 사용하여 계산되어진다. 또한, 유도가열조리기의 온도특성을 스테인레스와 알루미늄 각각에 대하여 주파수와 투자율에 따라 제시하였다.

Key Words : induction heating, FEM, IH-Jar, eddy current, input frequency

1. Introduction

Induction heating processes for heating provide significant technological, economic and ecological advantages in comparison with conventional oil or gas-fired furnace : fast heating rate, instant controllability, high efficient and minimal environment pollution.[1]-[3]
Therefore induction heating is widely used in today's industry, in operations such as metal hardening, preheating for forging operations, or cooking. It is a complex process involving both electromagnetic and thermal phenomena. Recently, induction heating Jar (IH-Jar) is very interested for high efficiency, the quickness of heating time and the convenient regulation of heating spot. The magnetic field intensity and the heat source in the IH-Jar should be exactly calculated in order to make temperature distribution required on the surface of the IH-Jar. But, the waste of time and cost has been increased because the design method of the IH-Jar in the industry is depending on the experience. Therefore, it is continuously required that the development of precision design method is based on the exact magnetic field intensity and heat source. And, numerical simulation of IH-Jar clearly involves two coupled phenomena : electromagnetism and heating. An efficient eddy current computation

* 정회원 : 삼척대학교 소방방재공학과 겸임교수, 工博
245-711/강원도 삼척시 교동 산 253번지
email : ohhong@dreamwiz.com

* Part-Time Lecture, Dept. of Fire & Disaster Engineering, Samchok National University.

has to be performed in order to obtain the source term to be plugged into the heat equation.[4]-[7]

In this paper, the magneto-thermal analysis of the IH-Jar was presented as an efficient design. The magnetic field intensity inside the axisymmetric shaped cooker was analyzed using three-dimensional axisymmetric finite element method(FEM) and the effectual heat source was obtained by ohmic losses from eddy currents induced in the IH-Jar. The heat was calculated using the heat source and heating equation. Also, it was represented the temperature characteristics of the IH-Jar according to input frequency and relative permeability in stainless parts and in aluminum parts.

2. The Three-dimensional Axisymmetric FEM of IH-Jar

The construction of the IH-Jar can apply to the three-dimensional axisymmetric FEM because it is the same form for circular direction. We can summarize the Maxwell's equation describing the systems with eddy currents as follows equation (1)~(5).

$$\nabla \times H = J \tag{1}$$

$$J = \sigma E \tag{2}$$

$$E = -\frac{\partial A}{\partial t} - \nabla \phi \tag{3}$$

$$B = \nabla \times A \tag{4}$$

$$B = \mu H \tag{5}$$

where H is the intensity of magnetic field, J is the sinusoidal exciting current density, σ is the electric conductivity of mass, E is the intensity of electric field, A is the magnetic vector potential, ϕ is the scalar potential, B is the magnetic flux density and μ is the permeability of mass. For the system, we can set the $\nabla \phi$ in equation(3) to zero[7], the final governing equation for A is the equation(6).

$$\frac{1}{\mu} \nabla^2 A = j\omega\sigma A - J \tag{6}$$

where ω represents the angular input frequency of the sinusoidal exciting current. The energy functional whose Euler-Lagrange equation is the same as governing equation(6) can be expressed as equation(7).

$$F = \int_S \frac{1}{2\mu} \left\{ \left(\frac{1}{r} \frac{\partial rA}{\partial z} \right)^2 + \left(\frac{1}{r} \frac{\partial rA}{\partial r} \right)^2 \right\} 2\pi r dr dz + \frac{j\omega}{2} \int_S \sigma A^2 \, 2\pi r dr dz - \int_S JA \, 2\pi r dr dz \tag{7}$$

After discretizing of the system, minimization condition of the energy functional equation(7) gives the system matrix equations(8).

$$[P]\{A\} + [Q]\{A\} = \{R\} \tag{8}$$

where [P] and [Q] are the coefficient matrices and {R} is the forcing vector. The coefficient matrices and the forcing vector can be assembled with element matrices written as equation(9)~(11).

$$[P]^e = \frac{1}{4\mu^e \triangle^e} \begin{bmatrix} b_l^2 + c_l^2 & b_l b_m + c_l c_m & b_l b_n + c_l c_n \\ b_l b_m + c_l c_m & b_m^2 + c_m^2 & b_m b_n + c_m c_n \\ b_l b_n + c_l c_n & b_m b_n + c_m c_n & b_n^2 + c_n^2 \end{bmatrix} \tag{9}$$

$$[Q]^e = \frac{j\omega\sigma^e \triangle^e}{12} \begin{bmatrix} 2 & 1 & 1 \\ 1 & 2 & 1 \\ 1 & 1 & 2 \end{bmatrix} \tag{10}$$

$$[R]^e = \frac{J^e \triangle^e}{3} \begin{bmatrix} 1 \\ 1 \\ 1 \end{bmatrix} \tag{11}$$

where $\triangle^e$ is the area of that element.

It can be calculated the magnetic vector potential, the eddy current and the heat source in each node by solving the system matrix equation. And the eddy current, J_e , is the equation(12) from ohms law as shown below.

$$J_e = \sigma E_e = -\sigma \frac{\partial A}{\partial t} = -j\omega\sigma A \qquad (12)$$

The heat source per unit volume, $ht_s[W/m^3]$, is written as equation(13).

$$ht_s = \frac{|J_e|^2}{\sigma} = \omega^2 \sigma |A|^2 = \omega^2 \sigma A A^* \qquad (13)$$

3. The Magnetic Analysis of IH-Jar

Table 1 and figure 1 are respectively the three-dimensional axisymmetric FE-model of the IH-Jar and the material constants of it.
Figs. 2, 3 and 4 are respectively the flux lines of case 1($\mu_r = 1$) , of case 2($\mu_r = 100$) and of case 3(. $\mu_r = 200$). Here we know that the flux lines cannot completely pass through the inner IH-Jar because of the skin effect of the stainless steel.

Table. 1 The material constants of the IH-Jar

	Stainless Steel	Aluminum
Relative permeability (μ_r)	1(case 1) 100(case 2) 200(case 3)	0.25×10^{-7}
Electric conductivity (σ)	1.66667×10^{6}	4.0×10^{7}
Thermal conductivity (k)	30	204

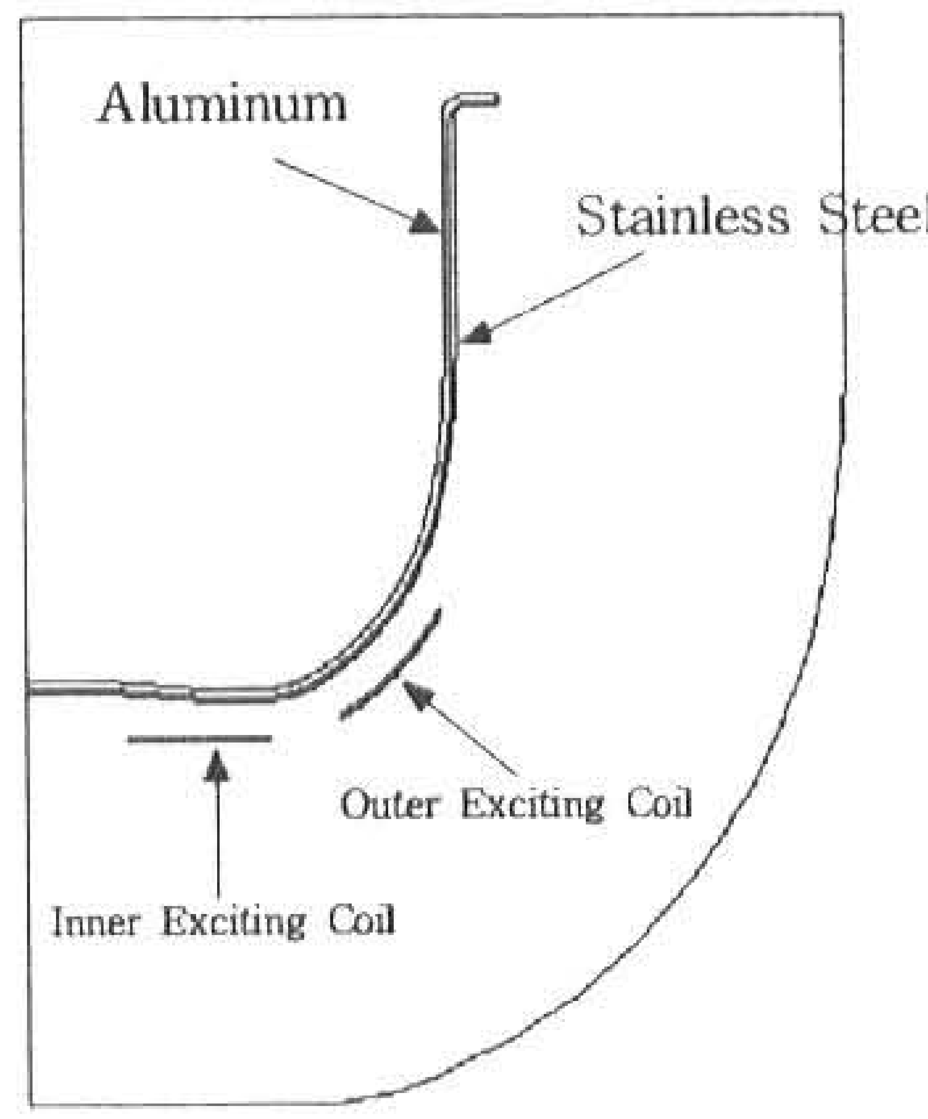

Fig. 1. The FE-model of the IH-Jar

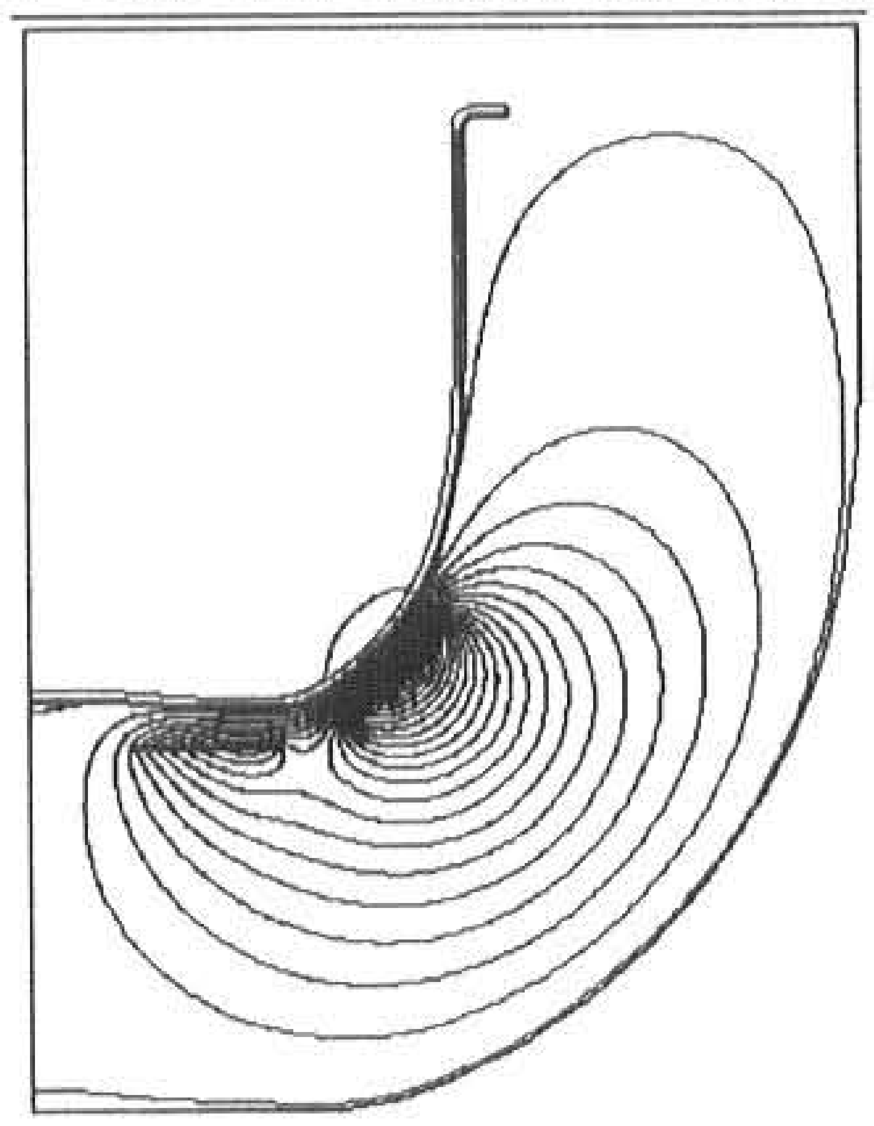

(Input frequency=25[kHz], $\mu_r = 1$)

Fig. 2. The flux lines of the IH-Jar

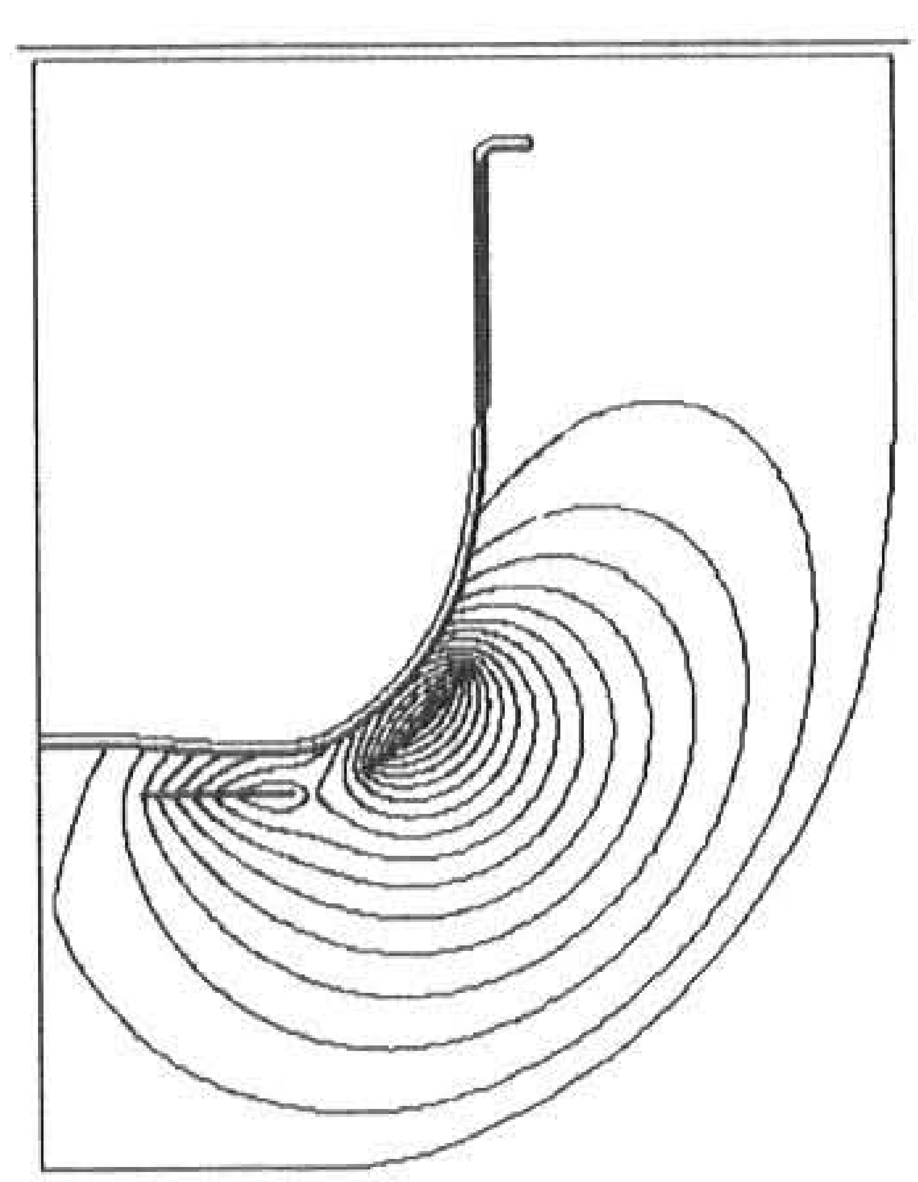

(Input frequency=25[kHz], $\mu_r = 100$)

Fig. 3. The flux lines of the IH-Jar

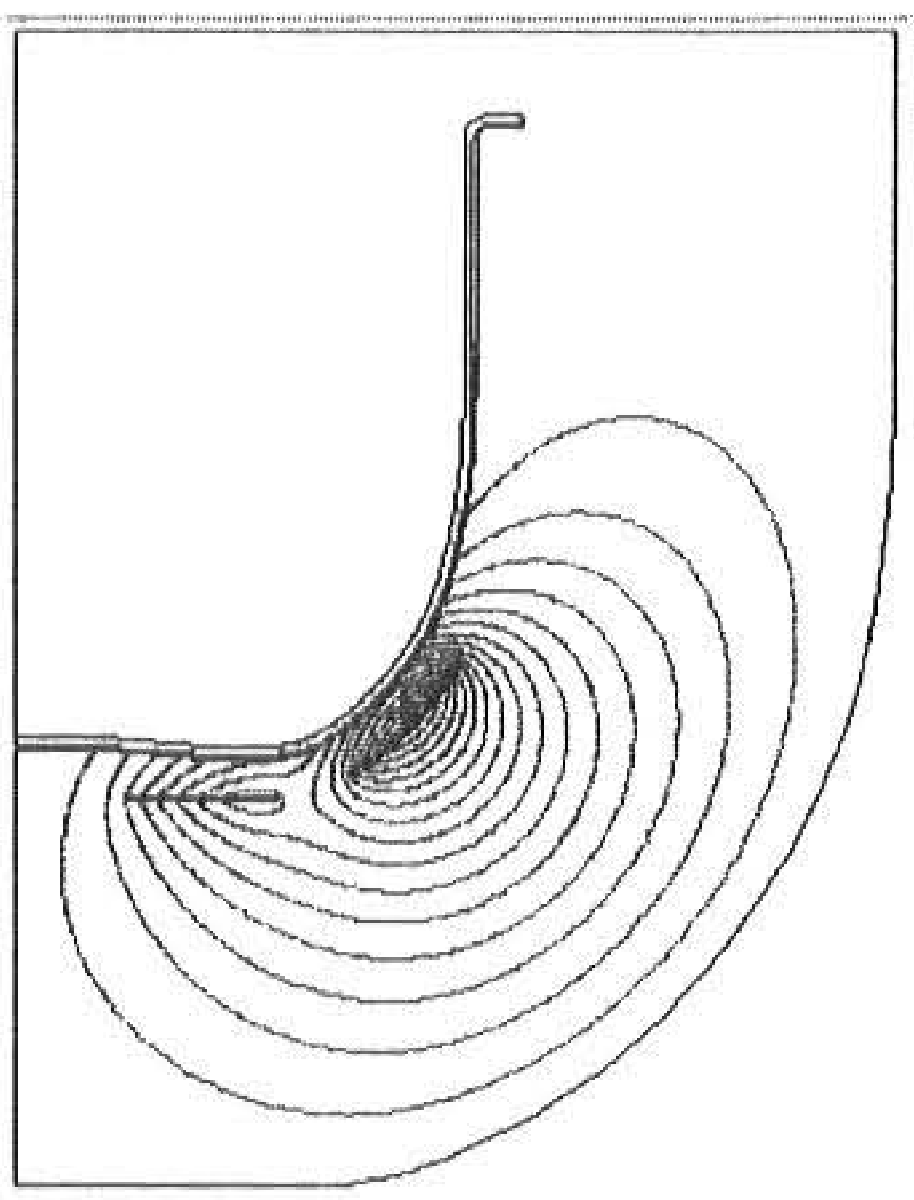

(Input frequency=25[kHz], $\mu_r = 200$)

Fig. 4. The flux lines of the IH-Jar

4. The Heat Analysis of the IH-Jar

The three-dimensional axisymmetric heat conduction equation in the steady state is expressed as follow:

$$\frac{1}{r}\frac{\partial}{\partial r}(kr\frac{\partial T}{\partial r}) + \frac{\partial}{\partial z}(k\frac{\partial T}{\partial z}) = -ht_s \quad (14)$$

where ht_s is the heat sources and k is the thermal conductivity. The complex boundary condition between the surface of the IH-Jar and the area around it is described by equation (15).

$$-k\frac{\partial T}{\partial n} = h(T - T_\infty) \quad (15)$$

where h is the convective exchange coefficient, T is the temperature in the boundary surfaces, T_∞ is the temperature of the fluid and $\frac{\partial T}{\partial n}$ is the normal component of the temperature in boundary surfaces. Arranging equation (14), we obtain equation (16).

$$-\frac{\partial}{\partial r}(r\frac{\partial T}{\partial r}) - \frac{\partial}{\partial z}(r\frac{\partial T}{\partial z}) = r\frac{ht_s}{k} \quad (16)$$

The heat conduction equation can be obtained with the standard Galerkins method as follows.

$$\int\int_A \left\{ r(\frac{\partial T}{\partial r})^2 + r(\frac{\partial T}{\partial z})^2 \right\} 2\pi r dr dz = \int\int_A 2Tr(\frac{ht_s}{k}) 2\pi r dr dz \quad (17)$$

And the element matrix can be expressed by the equations (18), (19) and (20).

$$K^e T^e = f^e \quad (18)$$

$$K^e_{ij} = \frac{\pi}{2\Delta^e} r_0{}^2 (c_i c_j + d_i d_j) \quad (19)$$

$$f^e_i = \frac{\pi r_0 \Delta^e}{6} \frac{ht_s}{k} (2r_i + r_j + r_k) \quad (20)$$

where r_0 is $(r_1 + r_2 + r_3)/3$.

Also, the element matrix equation in the complex boundary is expressed as follows:

$$[K^e + \overline{K^e}] T^e = [f^e + \overline{f^e}] \quad (21)$$

where,

$$\overline{K^e} = \int_{A^e_2} \sigma N^{et} N^e dS \quad (22)$$

$$\overline{f^e} = \int_{A^e_2} g N^{et} dS \quad (23)$$

where σ is h/k, g is hT_∞/k and A^e_2 is the elements on the boundary with the complex boundary condition.

If σ is constant inside an element and the opposite side of node $i-th$ is the complex boundary surface, the equations (22) and (23) can be respectively expressed in terms of equations (24) and (25).

$$[\overline{K^e}]_i = \frac{\pi\sigma(c_i^2 + d_i^2)^{1/2}}{6} \times \begin{bmatrix} 3r_k + r_j & 0 & r_k + r_j \\ 0 & 0 & 0 \\ r_k + r_j & 0 & r_k + 3r_j \end{bmatrix} \quad (24)$$

$$[\overline{f^e}]_i = \frac{\pi g(c_i^2 + d_i^2)^{1/2}}{3} \begin{bmatrix} 2r_k + r_j \\ 0 \\ r_k + 2r_j \end{bmatrix} \quad (25)$$

Substituting equation (21) into equations (24) and (25), we can obtain the element matrix with the complex boundary condition. If the system matrix is constructed using the above equations and it is solved, the temperature in each node can be obtained.

5. Temperature Characteristics according to Input Frequency Variation

Figs. 5 and 6 represent respectively the temperature characteristics of the IH-Jar according to input frequency and relative permeability in stainless steel parts and in aluminum parts.

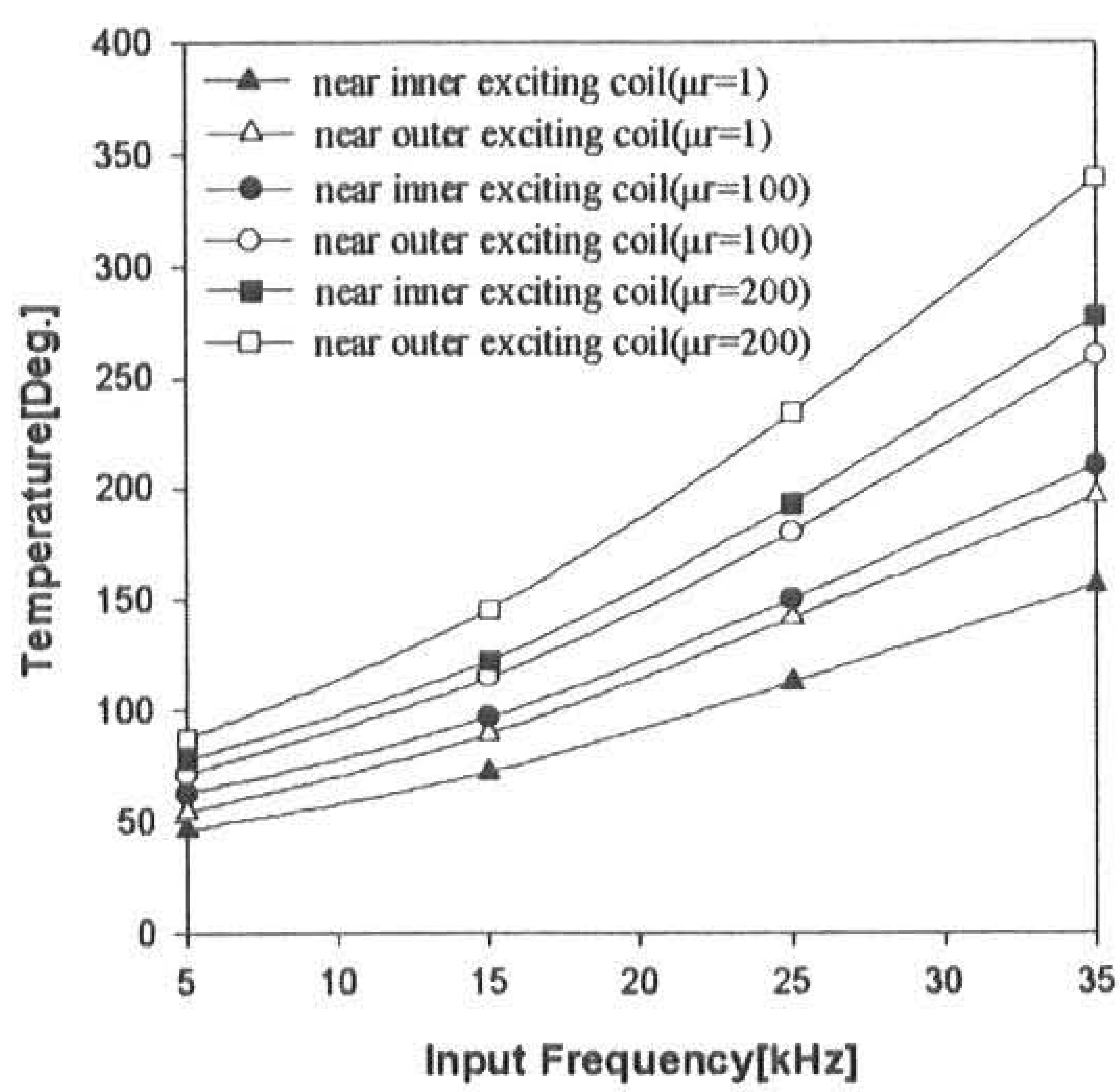

Fig. 5 The temperature curve of the IH-Jar in stainless steel.

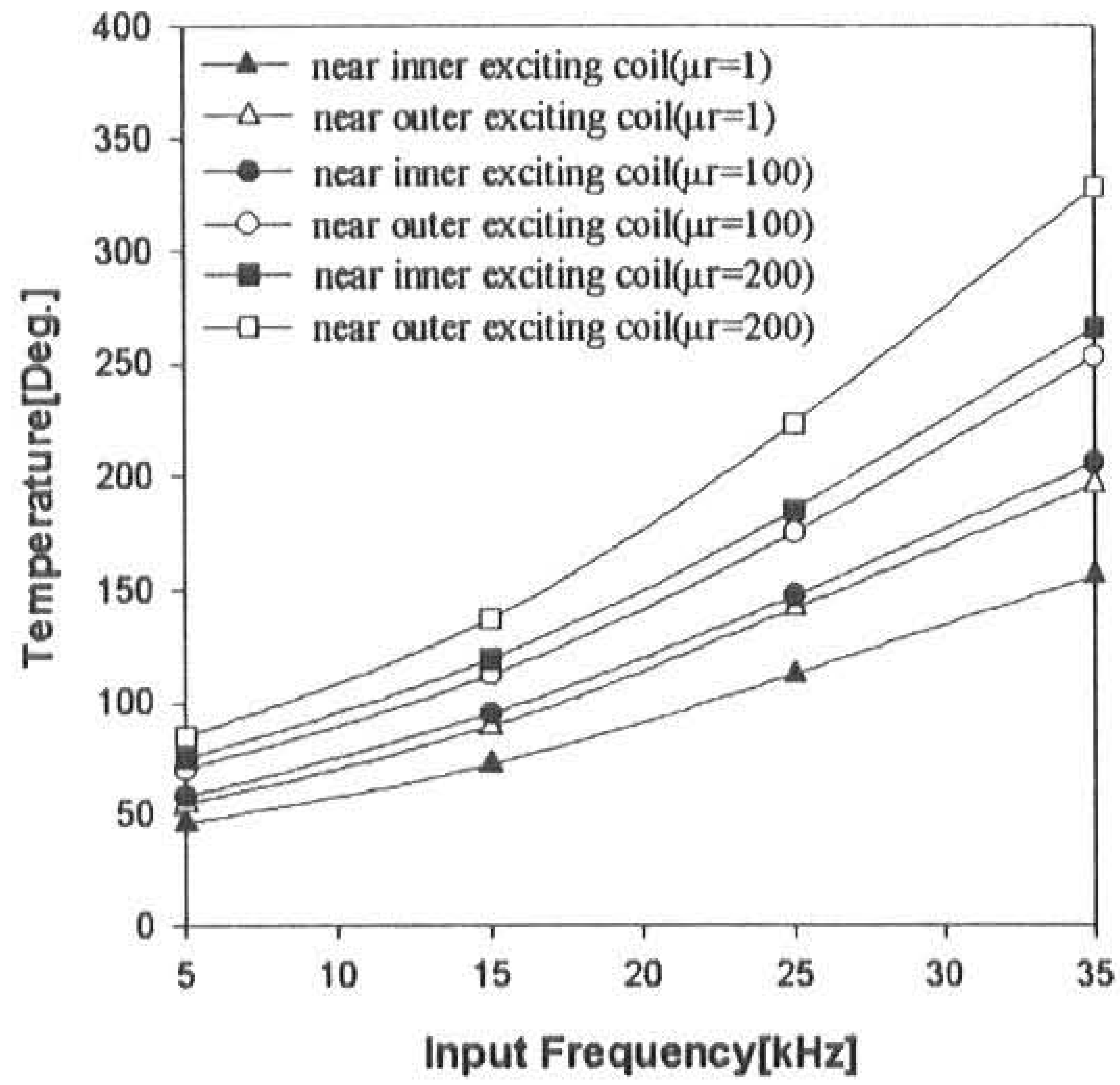

Fig. 6 The temperature curve of the IH-Jar in aluminum.

we know that the temperature of aluminum is higher than that of stainless steel at point distant from the heat source because the thermal conductivity of aluminum is larger than that of stainless steel. Also we know that the temperature of the IH-Jar is rapidly reached its peak value as the value of relative permeability and of input frequency are high. The temperature of the IH-Jar at near the outer exciting coil is larger than that at its near inner exciting coil.

6. Conclusions

In this paper, the magneto-thermal of IH-Jar was analyzed using three-dimensional axisymmetric finite element method(FEM).

And the heat was calculated using the heat source and heating equation. Also, it was represented the temperature characteristics of the IH-Jar according to input frequency and relative permeability in stainless parts and in aluminum parts. The temperature of aluminum is higher than that of stainless steel at point distant from the heat source because the thermal conductivity of aluminum is larger than that of stainless steel. Also we know that the temperature of the IH-Jar is rapidly reached its peak value as the value of relative permeability and of frequency are high. The temperature of the IH-Jar near the outer exciting coil is larger than that at its near inner exciting coil.

References

1) Zanming Wang, Xiaoguang Yang, Youhua Wang and Weili Yan, "Eddy Current and Temperature Field Computation in Transverse Flux Induction Heating Equipment for Galvanizing Line" , IEEE Trans. on Mag., Vol.37, No.5, pp.3437-3439, 2001.

2) Piotr Urbanek, Adam Skork, "Magnetic Flux and Temperature Analysis in Induction Heated Steel Cylinder" , IEEE Trans. on Mag., Vol.30, No.5, pp.3328-3330, 1994.

3) Yoshihiro Kawase, Tsutomu Miyatake, Katsuhiro Hirata, "Thermal Analysis of Steel Blade Quenching by Induction Heating" , IEEE Trans. on Mag., Vol.36, No.4, pp.1788-1791, 2000.

4) Masato Enokizono, Takashi Todaka, Shotaro Nishimura, "Finite Element Analysis of High-Frequency Induction Heating Problems Considering Inhomogeneous Flow of Exciting Currents" , IEEE Trans. on Mag., Vol.35, No.3, pp.1646-1649, 1999.

5) C. Chaboudez, S. Clain, R. Glardon, etc., "Numerical Modeling in Induction Heating for Axisymmetric Geometries", IEEE Trans. on Mag., Vol.33, No.1, pp.739-745, 1997.

6) Zs. Badics, H. Riedler, H. Stogner, "Application of FEM to Coupled Electric, Thermal and Mechanical Problems" , IEEE Trans. on Mag., Vol.30, No.5, pp.3316-3319, 1994.

7) Tanroku Miyoshi, Munehiko Sumiya, Hideki Omori, "Analysis of an Induction Heating System by Finite Element Method" , T.IEE Japan, RM-86-53, PP.117-125, 1986.

8) Tatsuya FURUKAWA, Itsuya MUTA and Tatsuhiko KOSUGI, "Finite Element Analysis of Induction Heating Range" , Reports of the Faculty of Science and Engineering, Saga University, PP. 81-87, 1988.

9) Hong-Seok Oh, etc., "A Study on the Heat-Diffused Prediction of Induction Heating Jar using Finite Element Method", International conference IEB, pp.234-240, 2002.

(2002년 5월 20일 접수, 2002년 8월 20일 채택)